Applied Energy 190 (2017) 135–146

Contents lists available at ScienceDirect

Applied Energy

journal homepage: www.elsevier.com/locate/apenergy

Underground pumped storage hydropower plants using open pit mines: How do groundwater exchanges influence the efficiency?

Estanislao Pujades [a,*], Philippe Orban [a], Sarah Bodeux [a], Pierre Archambeau [b], Sébastien Erpicum [b], Alain Dassargues [a]

[a] Hydrogeology and Environmental Geology, Geo3, Dpt ArGEnCo, Aquapole, University of Liege, 4000 Liege, Belgium
[b] Hydraulics in Environmental and Civil Engineering (HECE), Dpt ArGEnCo, Aquapole, University of Liege, 4000 Liege, Belgium

HIGHLIGHTS

- UPSH allows storing (and producing) large amounts of energy in flat regions.
- UPSH plants interact with the surrounding porous media exchanging water.
- Water exchanges influence the head difference between reservoirs.
- Efficiency of UPSH plants is affected by the water exchanges.
- Higher water exchanges improve the efficiency of pumps and turbines.

ARTICLE INFO

Article history:
Received 30 July 2016
Received in revised form 16 December 2016
Accepted 17 December 2016
Available online 3 January 2017

Keywords:
Pumped storage
Hydropower
Energy storage
Open pit
Efficiency
Groundwater

ABSTRACT

Underground Pumped Storage Hydropower (UPSH) is a potential alternative to manage electricity production in flat regions. UPSH plants will interact with the surrounding porous medium through exchanges of groundwater. These exchanges may impact the surrounding aquifers, but they may also influence the efficiency of the pumps and turbines because affecting the head difference between the reservoirs. Despite the relevance for an accurate efficiency assessment, the influence of the groundwater exchanges has not been previously addressed.

A numerical study of a synthetic case is presented to highlight the importance of considering the groundwater exchanges with the surrounding porous medium. The general methodology is designed in order to be further applied in the decision making of future UPSH plants introducing each case specific complexity. The underground reservoir of a hypothetical UPSH plant, which consists in an open pit mine, is considered and modelled together with the surrounding porous medium. Several scenarios with different characteristics are simulated and their results are compared in terms of (1) head difference between the upper and lower reservoirs and (2) efficiency by considering the theoretical performance curves of a pump and a turbine. The results show that the efficiency is improved when the groundwater exchanges increase. Thus, the highest efficiencies will be reached when (1) the underground reservoir is located in a transmissive porous medium and (2) the walls of the open pit mine do not constrain the groundwater exchanges (they are not waterproofed). However, a compromise must be found because the characteristics that increase the efficiency also increase the environmental impacts. Meaningful and reliable results are computed in relation to the characteristics of the intermittent and expected stops of UPSH plants. The frequency of pumping and injection must be considered to properly configure the pumps and turbines of future UPSH plants. If not, pumps and turbines could operate far from their best efficiency conditions.

1. Introduction

Over 81% of the total energy consumed in the world, of which ≈58% is represented by electricity generation in the countries members of the Organisation for Economic Co-operation and Development (OECD), is obtained from fossil fuels [1]. This depen-

* Corresponding author.
E-mail addresses: estanislao.pujades@gmail.com, estanislao.pujades@ulg.ac.be (E. Pujades).

http://dx.doi.org/10.1016/j.apenergy.2016.12.093
0306-2619/

dence is not sustainable because fossil fuels are limited and impact the environment (e.g., the greenhouse effect). It is therefore necessary to develop renewable sources of energy to replace the electricity obtained from fossil fuels in the near future.

The most important concern with respect to some forms of renewable energy, such as solar and wind energies, is their intermittence and the fact that their production over time cannot be matched to variations in demand [2–6]. Therefore, energy storage systems have become the key to improve the efficiency of renewable energy and increase its utilization [7]. Energy storage systems allow the production of electricity to be managed according to the demand [8,9]. These systems allow the excess energy to be stored during low demand periods and producing electricity when the demand increases.

Pumped Storage Hydropower (PSH) is one of the most commonly used storage systems [10] because it allows large amounts of electricity to be stored and produced [11]. PSH plants, which consist of two reservoirs located at different heights, allow a large percentage (≈70%) of the excess electricity generated during the low demand periods to be reused [12]. However, PSH technology is constrained by topography and land availability because it requires a minimum elevation difference between the two reservoirs as well as large volumes [13]. In addition, PSH plants are controversial due to their impacts on landscape, land use, environment (vegetation and wildlife) and society (relocations) [14,15].

Conversely, Underground Pumped Storage Hydropower (UPSH) [16] is an alternative to store and manage large amounts of electricity that is not limited by topography. Consequently, more sites are available [17]. UPSH plants consist of two reservoirs; the upper reservoir is located at the surface or at shallow depth, while the lower reservoir is underground. Although the underground reservoir can be drilled [18], the cheapest (and possibly most efficient) alternative consists of using abandoned works, such as deep or open pit mines [19,20]. Impacts on land use, vegetation and wildlife produced by UPSH are lower than those of PSH because (at least) one of the reservoirs is underground. However, it is needed to consider the effects of UPSH plants on surrounding porous media to quantify the total environmental impact. Social impacts of UPSH plants are also lower because (1) less relocations are required (the lower reservoir is underground) and (2) the reuse of abandoned mines contributes adding value to local communities after the cessation of mining activities. In addition, sedimentation problems should be also lower in UPSH plants because used groundwater is filtered by the porous medium. Sedimentation problems could probably appear by eroded materials from the open pit walls.

Despite of the benefits, there are no bibliographic evidence of UPSH plants constructed. However, some studies and projects have been mentioned and developed until now. During 1980's a project to install an UPSH plant was launched in the Netherlands [21], but the plant was not finally constructed for different reasons such as the inadequate characteristics of the soil [22]. Wong [14] assessed the possibility of construct UPSH plants in Singapore using abandoned rock quarries as upper reservoirs. In this case, Wong [14] proposed to drill tunnels or shafts to be used as underground reservoirs. Severson [23] evaluated the potential of ten sites to stablish an underground taconite mine in Minnesota (USA) whose cavity would be after used as lower reservoir for an UPSH plant. Some preliminary studies have been also carried out in Germany to assess the possibilities for construct UPSH plants on abandoned mines in the Harz and Ruhr regions [24–26]. Finally, Spriet [22] explored the possibility for constructing an UPSH plant in Martelange (Belgium).

Underground works are rarely isolated, and groundwater exchanges between UPSH plants and the surrounding porous medium will occur if they are used as underground reservoirs. In addition to the impacts on groundwater levels [20,27], groundwater exchanges may affect the efficiency of UPSH plants. The efficiency of the pumps and turbines depends on the head difference between the upper and the lower reservoirs. This head difference, which varies over time and can be easily predicted in PSH plants (i.e. with waterproof reservoirs), may be influenced by the groundwater exchanges in UPSH plants. Therefore, it is crucial to determine the influence of these exchanges on the head difference between the reservoirs and consequently on UPSH efficiency. This would allow the efficiency of future UPSH plants to be improved by selecting pumps and turbines adapted to the effective groundwater exchanges with the surrounding porous medium. However, no studies in the literature have focused on this issue.

In this study, a synthetic case of an UPSH plant that utilizes an open pit mine as underground reservoir is considered, and the relationship between the groundwater exchanges and the efficiency of the pumps and turbines is studied numerically. The influence of groundwater exchanges on the efficiency and how this varies depending on the system properties (porous medium parameters, open pit mine characteristics and pumping/injection features) are investigated. The main objective is to highlight the paramount importance of considering groundwater exchanges during the design stage of future UPSH plants.

2. Materials and methods

2.1. Problem statement

The problem is formulated as shown in Fig. 1. A hypothetical UPSH plant whose underground reservoir is an open pit mine is considered. Of course, actual properties of open pit mines are more complex, but the goal of the paper is, at this stage, to assess the general relevance of groundwater exchanges in terms of efficiency. Still, some characteristics of the adopted geometry (e.g. the mine flooded depth) are similar to some actual geometries of open pit lakes in Western Europe [28]. The geometry of the open pit mine is conceptually simplified as a square cuboid (top and bottom faces are squares) with a depth of 100 m to facilitate the numerical study while obtaining representative results. This geometrical simplification may affect the volume of groundwater exchanges but not the assessment of their influence on the efficiency of UPSH plants. The initial hydraulic head under natural conditions (without pumping or injection) is located at a depth of 50 m. As a result, half of the open pit is saturated.

The whole thickness (100 m) of the surrounding porous medium is assumed homogeneous and isotropic. The water table is located at a depth of 50 m. Therefore, under natural conditions, it is a 50-m-thick unconfined porous medium. The numerical model has a flat geometry for representing a typical horizontal layered geology. The external boundaries are chosen located at 2500 m from the reservoir to minimize their impact on the simulated evolution of the hydraulic head inside the open pit mine. Their impacts are lower and are later observed as further the boundaries are located. Additional simulations were performed reducing the length of the model to ensure that the flat shape of the modelled domain does not affect the results.

The evolution of the hydraulic head in the underground reservoir is computed to assess the differences between the simulations. Given that the objective is to assess the impact of the groundwater exchanges on the efficiency, a very large and shallow upper reservoir is assumed to eliminate its influence on the results (i.e., the increments of the head difference in the upper reservoir produced by its repeated filling and emptying are neglected). Consequently, the computed head difference is only based on the evolution of the hydraulic head in the underground reservoir.

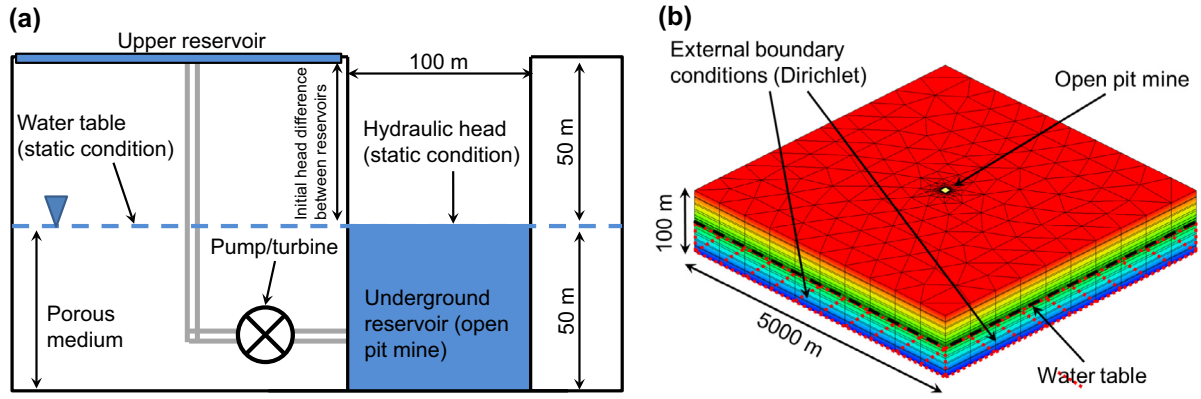

Fig. 1. (a) Sketch of the cross section of the problem. (b) View of the numerical model. The red dashed lines highlight the area where the Dirichlet BCs are prescribed. The saturated zone of the model is located below the water table. (For interpretation of the references to colour in this figure legend, the reader is referred to the web version of this article.)

Actual frequency of pumping and injection phases of future UPSH plant cannot be forecasted because it depends on a lot of factors (day, season, meteorological conditions if wind or solar energies are the main energy resources, electrical smart grid optimization scenarios. . ..). Thus, to obtain representative results, the frequency adopted in most of the simulations was deduced from a 1 year actual electricity price curve [27] where it is possible to observe that there are two peaks of electricity price the most of the days. Consequently, the simulated pumping and injection phases have durations of 0.25 day. Five theoretical hypotheses are considered for the frequency/intermittence of the pumping and injection. Fig. 2 shows the evolutions of the 5 pumping and injection rates over the first five simulated days. For one hypothesis, the frequency, duration and rates of pumping and injection are kept constant for the entire simulation time (500 days). The first hypothesis consists of continuous pumping and injection (stops are not considered). Periods of inactivity are considered in Hypotheses 2–5. Hypothesis 2 considers a 0.5 day period of inactivity after each injection, Hypothesis 3 considers 0.5 days of inactivity after each pumping phase, Hypothesis 4 considers 1 day of inactivity after every two injection phases, and Hypothesis 5 considers 1 day of inactivity after every two pumping phases. The pumping and injection rates are 2 m^3/s, and the mean hydraulic power is thus 1 MW. In contrast to reality, the considered pumping/injection hypotheses are not complex. Nevertheless, these scenarios allow the main trends of the system to be determined.

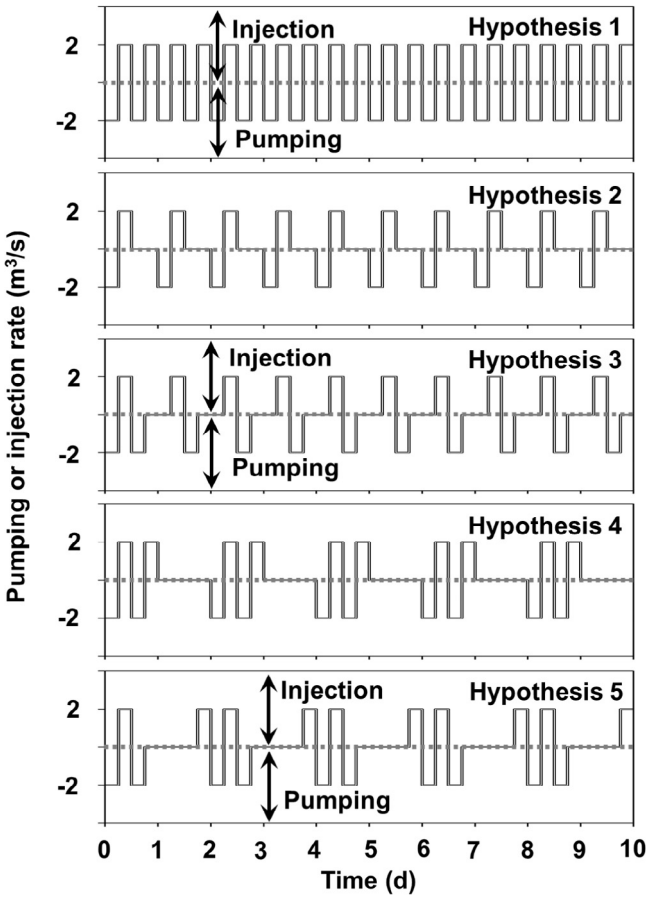

Fig. 2. Evolutions of the pumping and injection rates (m^3/s) considered in the simulations. Negative values mean that water is extracted (pumped), while positive values mean that water is released into the open pit mine.

2.2. Numerical model

The finite element numerical code SUFT3D [29,30] is used to model the underground reservoir and its interactions with the porous medium. This code uses the Control Volume Finite Element (CVFE) method to solve the groundwater flow equation based on the mixed formulation of Richard's equation proposed by Celia et al. [31]:

$$\frac{\partial \theta}{\partial t} = \underline{\nabla} \cdot \underline{\underline{K}}(\theta) \cdot \underline{\nabla} h + \underline{\nabla} \cdot \underline{\underline{K}}(\theta) \cdot \underline{\nabla} z + q \quad (1)$$

where θ is the water content [–], t is the time [T], $\underline{\underline{K}}$ is the hydraulic conductivity tensor [LT^{-1}], h is the pressure head [L], z is the elevation [L], and q is a source/sink term [T^{-1}]. Fig. 1b shows an image of the numerical model. The mesh is made up of prismatic 3D elements and is divided vertically into 16 layers, whose respective thicknesses are reduced in the zone around the initial water table. The layers near the water table are 1 m thick, while the top and bottom layers are 10 m thick. The horizontal size of the elements decreases towards the underground reservoir (from 500 m near the boundaries to 10 m in the centre of the domain). The validity of the mesh has been tested by ensuring that results are not sensitive to mesh refinements.

The underground reservoir is modelled as a linear reservoir and is discretized as a single mixing cell. The velocity inside the mixing cell is neglected. An internal dynamic Fourier boundary condition (BC), which is a head-dependent BC, between the underground reservoir and the surrounding porous medium [30] is used to

simulate the groundwater exchanges. The internal Fourier BC is defined as follows:

$$Q_i = \alpha' A(h_{aq} - h_{ur}) \quad (2)$$

where Q_i is the exchanged flow [L^3T^{-1}], h_{aq} is the piezometric head in the porous medium [L], h_{ur} is the hydraulic head in the underground reservoir [L], A is the exchange surface [L^2], and α' is the exchange coefficient [T^{-1}], with $\alpha' = (K'/b')$, where K' and b' are the hydraulic conductivity [LT^{-1}] and the width [L] of the lining, respectively. Different lining conditions are considered by varying the value of α'; non-lined walls are simulated with high values of α'. Given that the maximum value of K' cannot be greater than the hydraulic conductivity of the porous medium (K), high values of α' allow simulating a very thin lining as conductive as the porous medium. It is possible to deduce from Eq. (2) that groundwater exchanges vary linearly as a function of the difference in water level between the reservoir and the surrounding porous medium [32].

The retention curve and the relative hydraulic conductivity are defined as follows (Yeh, 1987):

$$\theta = \theta_r + \frac{(\theta_s - \theta_r)}{h_b - h_a}(h - h_a) \quad (3)$$

$$K_r(\theta) = \frac{\theta - \theta_r}{\theta_s - \theta_r}, \quad (4)$$

where θ_s is the saturated water content [–], θ_r is the residual water content [–], K_r is the relative hydraulic conductivity [LT^{-1}], h_b is the pressure head at which the water content is the same as the residual water content [L], and h_a is the pressure head at which the water content is less than the saturated water content [L]. The parameters h_a and h_b are taken as 0 and −5 m, respectively, and are held constant in all of the scenarios. The law that is used to define the transition between the partially saturated and saturated zones is chosen for its linearity. It does not affect the results of this study, which focuses on the saturated zone, and eliminates convergence errors that can appear using other laws.

Dirichlet BCs are adopted at the external boundaries of the numerical model. These BCs consists of prescribing the piezometric head at a depth of 50 m (the same as the initial piezometric head). It is assumed that the volume of water provided by a hypothetical recharge or from a lower stratum is negligible. Consequently, no-flow BCs are adopted at the top and bottom boundaries.

A set of numerical simulations are performed, and their results are compared to assess the influence of the system variables on the efficiency. The assessed (and modified) variables are K, θ_s, the storage capacity of the open pit mine, α' and the frequency of the pumping and injection phases. The latter is achieved by considering the 5 hypotheses shown in Fig. 2.

2.3. Basic concepts

2.3.1. Evolution of the head difference between the upper and underground reservoirs

Fig. 3 shows the evolution of the head difference between the upper and the lower reservoirs for the entire time period (Fig. 3a) and during the first 10 simulated days (Fig. 3b). The head difference evolution is computed with the numerical model by considering a reference scenario with the following characteristics: K = 1 m/d, $\theta_s = 0.1$, α' = 1000 d^{-1} (i.e., no lining is simulated), and the pumping and injection phases are continuous (Hypothesis 1).

The head difference oscillates as a result of the water pumping and injection. The mid-range head difference, which is computed from the maximum and minimum head difference during each pumping and injection cycle, increases in the first cycle as a result of the first pumping phase and decreases progressively over time. After a period of time that depends on the characteristics of the problem, the mid-range head difference becomes constant, and a dynamic steady state is reached. The attained mid-range head difference depends on the pumping/injection hypothesis. In the simulated scenario, the mid-range head difference when the dynamic steady state is reached is the same as the initial head difference (50 m) because the adopted pumping/injection hypothesis is "symmetrical". The progressive decrease of the mid-range head difference is caused by the groundwater exchanges between the underground reservoir and the surrounding porous medium, which increases the hydraulic head in the reservoir. Groundwater flows in when the hydraulic head in the reservoir is lower than the piezometric head in the surrounding porous medium and flows out in the opposite situation. During the early cycles, most of the groundwater exchanges are inflows because the hydraulic head is lower than the piezometric head during longer time periods. The time interval of each cycle during which the hydraulic head is lower decreases progressively with increasing cycles, and after several cycles, this time interval lasts half of the cycle. At that moment, the hydraulic head is higher than the piezometric head during the other half of the cycle. When this occurs, the dynamic steady state has been reached, and the groundwater inflows and outflows during each cycle are the same. As a result of this behaviour, the rate of decrease of the mid-range head difference is higher at the beginning, and it decreases over time to 0.

The magnitude of the oscillations, the variation of the mid-range head difference and the time to reach the dynamic steady state depend on the system properties and are essential to study the impact of the groundwater exchanges on the UPSH efficiency.

2.3.2. Efficiency of pumps and turbines

For a constant rotation speed, the efficiency of pumps and turbines is defined by a pair of performance curves similar to those shown in Fig. 4 [33]. These curves relate the head difference and the efficiency with the pumping/injection rate. The best efficiency point (BEP), which is defined by the performance curves, is the point at which the efficiency is the maximum for a given head difference and pumping/injection rate. The head difference between the reservoirs, and therefore the efficiency, varies during the pumping and injection phases. As a result of this variation, pumps and turbines operate in a range of efficiencies that is called the "operation range". If the head difference defined by the BEP of the machine is consistent with the mid-range head difference, the BEP is centred with respect to the operation range. The efficiency increases as the operation range decreases. Therefore, higher efficiencies are reached when the change in the head differences between the reservoirs produced by the pumping and injection is smaller. It is also important to consider the variation of the mid-range head difference over time because it affects the efficiency. The efficiency only reaches its maximum value when the head difference defined by the BEP is consistent with the mid-range head difference. Therefore, if pumps and turbines are selected based on the mid-range head difference when the dynamic steady state is reached, the efficiency is lower at early times and increases progressively until achieving a maximum when the dynamic steady state is reached.

Groundwater exchanges between the open pit mine and the surrounding porous medium modify the hydraulic head inside the underground reservoir. Therefore, they may reduce or increase the operation ranges of the pumps and turbines and induce variations of the mid-range head difference over time. The efficiency will be higher when the magnitude of the oscillations and the variations of the mid-range head difference over time are lower. The time to reach the dynamic steady state should also be considered to assess the efficiency of UPSH plants. In the case of long stops

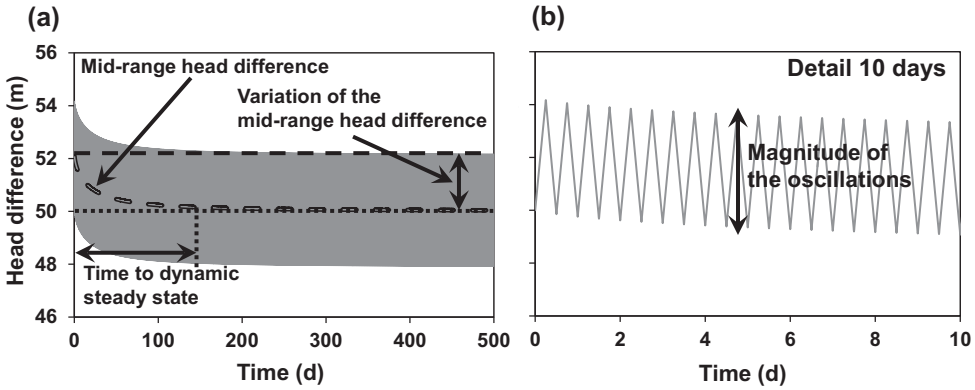

Fig. 3. (a) Evolution of the head difference between the upper and underground reservoirs over the entire simulated time. The dotted and dashed lines indicate the initial head difference between the reservoirs and the mid-range head difference during the first pumping/injection cycle, respectively. (b) Detail of the evolution of the head difference during the first 10 simulated days.

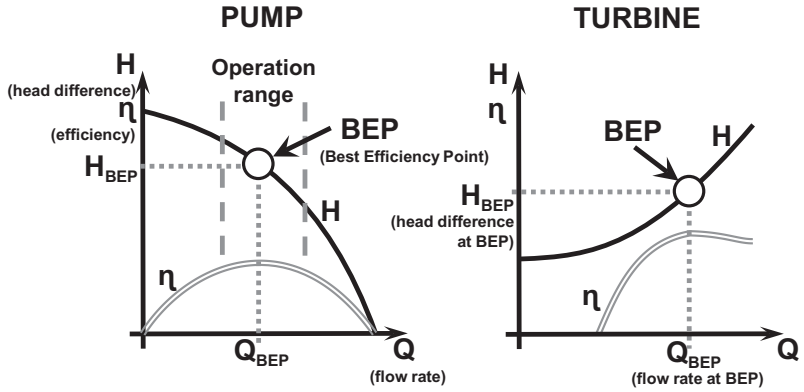

Fig. 4. Performance curves of pumps (left) and turbines (right). These curves define the best efficiency point (BEP). Pumps and turbines operate around the BEP (operation range). Modified from Chapallaz et al. [33].

(expected or not), during which the head difference between the reservoirs returns to its initial value, less time is required by the pumps and turbines to oscillate around the chosen BEP if the time to reach the dynamic steady state is shorter.

Actual performance curves of a pump and a turbine are used to support the numerical results of this study. The BEP defined by these performance curves is reached when the head difference is 50 m, which is consistent with the mid-range head difference when the dynamic steady state is reached assuming continuous pumping and injection cycles (Hypothesis 1) with a nominal pumping/injection rate of 2 m^3/s. The code used to model the groundwater flow does not allow the non-linear function that is defined by the performance curves and relates the pumping and injection rates to the head difference to be introduced. Therefore, performance curves of variable speed machines and a constant flow rate are used to assess the variations on the efficiency induced by groundwater exchanges. These curves, which are obtained from the performance curves of constant speed machines by applying the affinity laws of pumps and turbines [33], relate the speed of rotation and the efficiency with the head difference between the upper and lower reservoirs for a constant flow rate. Fig. 5 shows the performance curves for variable speed machines used in this study. Note that head losses are not considered. The equations that define these curves were derived by Microsoft Excel 2013. They served to compute analytically the efficiency by using the head difference obtained from the numerical model.

3. Results and discussions

3.1. Evolution of the average efficiency

Fig. 6 shows the average efficiency evolution for 5 scenarios (Sce1 to Sce5). One variable is modified in each scenario with respect to scenario 1 (Sce1) to determine its individual effect on the evolution of the average efficiency. The characteristics of Sce1 are as follows: $K = 1\ m^2/d$, $\theta_S = 0.1$, $\alpha' = 1000\ d^{-1}$, the saturated volume of the mine (V_{UR}) is 500,000 m^3, and Hypothesis 1 is considered for the pumping and injection phases. The value of K is 10 m/d in Sce2, θ_S is 0.2 in Sce3, α' is 0.01 d^{-1} in Sce4, and V_{UR} is 250,000 m^3 in Sce5.

Average efficiency shown in Fig. 6 is computed by the following steps: (1) a value of efficiency is calculated for each of the simulated time steps, which make up the pumping and injection phases, by using the head difference computed numerically and the performance curves displayed in Fig. 5; (2) the calculated efficiencies are averaged over each pumping and injection phase to obtain their average efficiency; and (3) the average efficiency over each pumping and injection phase is plotted versus time. Fig. 6 only shows the average value of the efficiency. Efficiency oscillations produced by pumping and injection, and therefore, the maximum and minimum efficiencies reached during each phase are not considered in this figure.

The average efficiency increases over time until it reaches a maximum and constant value. The maximum efficiency is reached

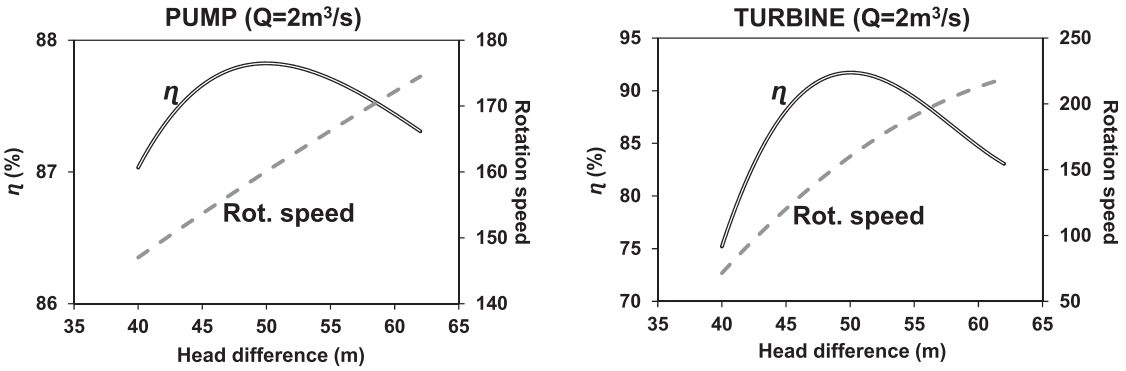

Fig. 5. Actual performance curves of the pump (left) and the turbine (right) considered in this study. The BEP is defined for a head difference of 50 m and a pumping/injection rate of 2 m^3/s.

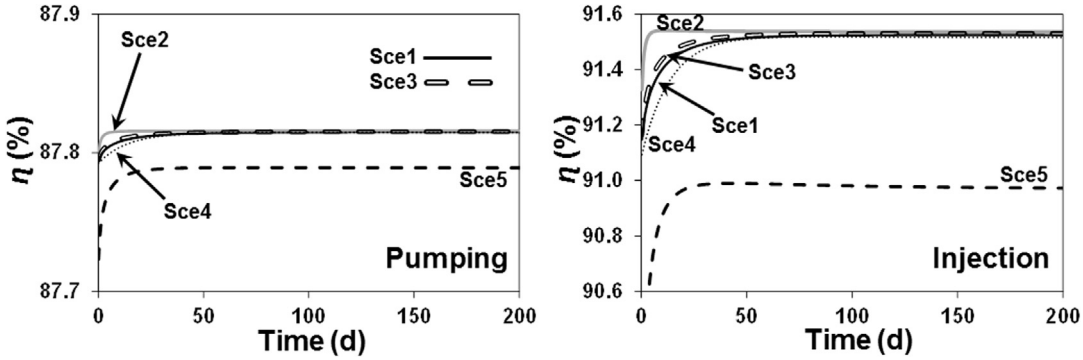

Fig. 6. Evolution of the average efficiency during the pumping (left) and injection (right) over 500 days for four simulated scenarios with different characteristics.

when the dynamic steady state is achieved and the mid-range head difference between the reservoirs is the same as the head difference defined by the BEP of the pump and the turbine. The lowest efficiencies are observed for Sce5 because the storage capacity of the underground reservoir is decreased in this scenario. Consequently, the magnitude of the oscillations, and therefore the operation ranges of the pump and the turbine, are higher.

The average efficiencies of scenarios Sce1 to Sce4 differ in the early times because the time required by the pump and the turbine to operate around their BEPs are different; it is shorter for Sce2 and longer for Sce4. This behaviour highlights the importance of the time required to reach the dynamic steady state to the efficiency in the case of long periods of inactivity. Pumps and turbines will need less time to operate around their BEPs if the dynamic steady state is reached more quickly. Note that if long periods of inactivity are frequent and the dynamic steady state is never reached, the efficiency could be improved by selecting pumps and turbines whose BEP is adapted to the head differences during the early cycles (higher than during the dynamic steady state).

Finally, the maximum efficiencies that are reached during the injection phases are not the same for scenarios Sce1 to Sce4. Higher efficiencies are reached for Sce2 because the magnitude of the oscillations, and therefore the operation ranges of the turbine, are smaller. Differences in the average efficiency of the pump are not observed because its performance curves are softer than those of the turbine. As a result, the efficiency of the pump varies less depending on the head difference.

3.2. Hydraulic conductivity of the porous medium (K)

The numerical results of 5 scenarios (Sce 6 to Sce10) with different values of K are summarized in Fig. 7. The common characteristics of these scenarios are as follows: $\theta_S = 0.1$, $\alpha' = 1000\ d^{-1}$, $V_{UR} = 500{,}000\ m^3$, and Hypothesis 1 is considered for the pumping and injection phases. The values of K are 0.1 m/d in Sce6, 1 m/d in Sce7, 10 m/d in Sce8, 100 m/d in Sce9 and 1000 m/d in Sce10.

Fig. 7a shows the head variations in the reservoir. The mid-range head difference, the magnitude of the oscillations and the time required to reach the dynamic steady state decrease with higher values of K. As a result, the pumps and turbines operate closer to the BEP in transmissive porous media (i.e. their efficiency is higher). The magnitude of the oscillations and the variation of the mid-range head difference are similar for values of K lower than 10 m/d. In these cases, the efficiency depends on the time required to reach the dynamic steady state. Fig. 7b shows the operation ranges for Sce6 to Sce10. These operation ranges are computed when the dynamic steady state is reached. The operation ranges of the pumps and turbines are smaller for higher values of K. Consequently, higher values of K improve the efficiency of the pumps and turbines. The operation ranges are similar for Sce6 to Sce8 because the groundwater exchanges and head variations are similar for values of K lower than 10 m/d. It is possible to calculate by using the performance curves (Fig. 5) the minimum efficiency reached during pumping and injection phases once the dynamic steady state is achieved. 87.2% (pumping) and 91.2% (injection) are the minimum efficiencies for Sce6, while 87.8% (pumping) and 91.7% (injection) are the minimum efficiencies for Sce10. These results corroborate that the efficiency of pumps and turbines is improved with higher K. These values are only illustrative because they will vary depending on the characteristics of pumps and turbines.

3.3. Storage coefficient of the surrounding porous medium

The influence of the storage coefficient of the surrounding porous medium (S) is assessed by varying θ_S in four scenarios (Sce11 to Sce14). Their common characteristics are as follows: $K = 1$ m/d,

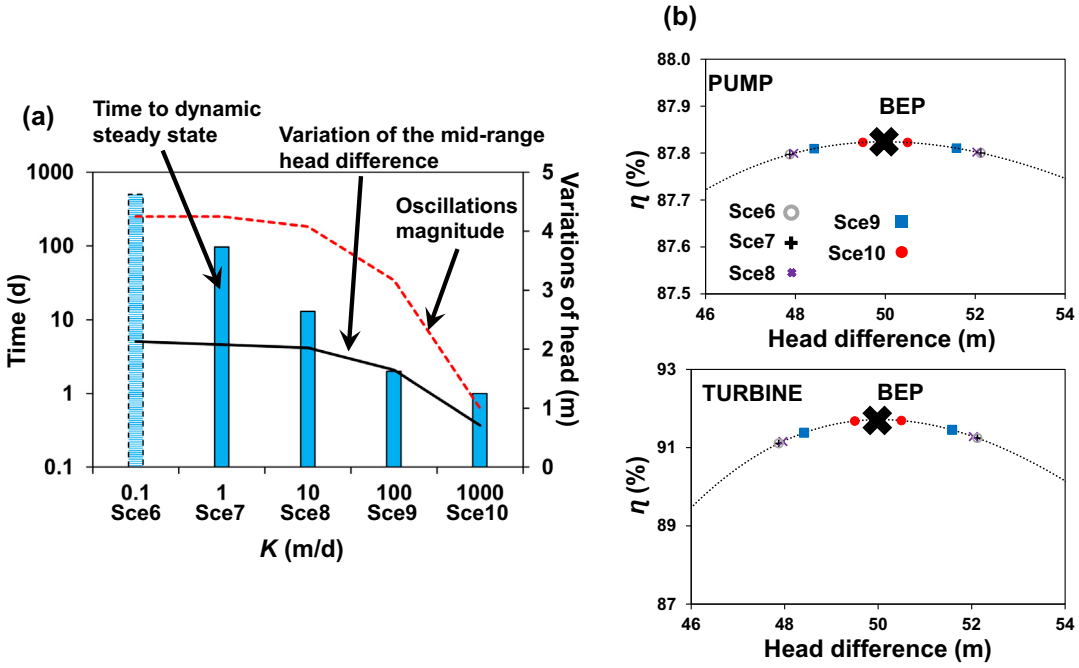

Fig. 7. (a) Head variations for 5 scenarios with different values of K of the porous medium. The background and contour line of the blue bar of Sce6 (K = 0.1 m/d) are different because the time to reach the dynamic steady state exceeds the simulated time. (b) Operation range when the dynamic steady state is reached for the simulated scenarios.

α' = 1000 d^{-1}, V_{UR} = 500,000 m^3, and Hypothesis 1 is considered for the pumping and injection phases. The values of θ_S are 0.05 in Sce11, 0.1 in Sce12, 0.2 in Sce13 and 0.3 in Sce14.

Fig. 8a summarizes the head variations. The groundwater exchanges increase with higher values of θ_S; however, this increase is relatively small, and the differences between the magnitudes of the oscillations and the variation of the mid-range head difference are negligible. Similar results are observed in Fig. 8b, which shows the operation ranges when the dynamic steady state is reached. The operation ranges are nearly the same for all scenarios (i.e., the symbols that represent each scenario overlap). The time to reach the dynamic steady state is the only characteristic that varies significantly between the scenarios. Thus, S modifies the time required by the pumps and turbines to operate around their BEPs. These results suggest that S is an important variable when long periods of inactivity, during which the head difference between

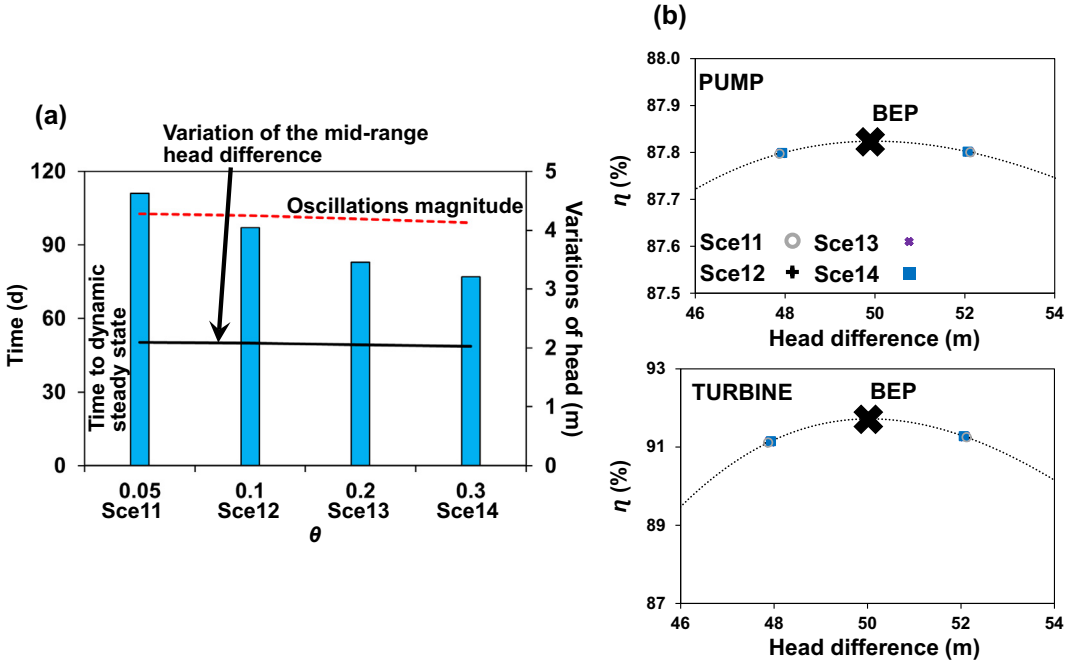

Fig. 8. (a) Head variations for 4 scenarios with different values of S of the porous medium. (b) Operation range when the dynamic steady state is reached for the simulated scenarios.

the reservoirs returns to its initial value, may occur. Less time is needed to reach the dynamic steady state and oscillate around the selected BEP when S decreases.

3.4. Exchange coefficient (α')

The influence of α' is evaluated by comparing the numerical results of six scenarios (Sce15 to Sce20). The common features of the scenarios are as follows: K = 10 m/d, $\theta_S = 0.1$, V_{UR} = 500,000 m^3, and Hypothesis 1 is considered for the pumping and injection phases. The values of α' are 0.01 d^{-1} in Sce 15, 0.1 d^{-1} in Sce16, 1 d^{-1} for Sce17, 10 d^{-1} in Sce18, 100 d^{-1} in Sce19 and 1000 d^{-1} in Sce20.

The head variations (Fig. 9a) and the operation ranges of the pumps and turbines (Fig. 9b) are similar in all of the scenarios. The most noticeable difference is in the time required to reach the dynamic steady state, which increases with lower values of α' (but not significantly). Although α' controls the groundwater exchanges, if the porous medium cannot provide enough water, its influence is not noticed. As shown in Fig. 7, the head differences are similar in scenarios Sce1, Sce2 and Sce3, which suggests that the groundwater exchanges are similar for values of K lower than 10 m/d. Therefore, head variations are similar in Sce15 to Sce20 because the groundwater exchanges are constrained by the porous medium. Thus, influence of α' is limited and groundwater exchanges do not vary significantly.

K is increased to 100 m/d in scenarios 21–26 to ascertain the influence of α'. The other common characteristics of the scenarios are: $\theta_S = 0.1$, V_{UR} = 500,000 m^3, and Hypothesis 1 is considered for the pumping and injection phases. The values of α' are 0.01 d^{-1} in Sce21, 0.1 d^{-1} in Sce22, 1 d^{-1} in Sce23, 10 d^{-1} in Sce24, 100 d^{-1} in Sce25 and 1000 d^{-1} in Sce26.

Fig. 10a and b shows the head variations and the operation ranges, respectively. The influence of α' is greater because the groundwater exchanges are constrained less by the porous medium properties. The magnitude of the oscillations, the variation of the mid-range head difference and the time to reach the dynamic steady state decrease with higher values of α' because the groundwater exchanges increase. Consequently, the operation ranges are smaller for higher values of α'. The head variations (magnitude of the oscillations and variation of the mid-range head difference) and operation ranges are similar for values of α' higher than 100 d^{-1} because the simulated interface between the porous medium and the underground reservoir is more conductive than the porous medium. In these situations, the groundwater exchanges are only constrained by the porous medium parameters, which are the same in all of the scenarios. Although the head variations and operation ranges are also similar for values of α' lower than 1 d^{-1}, the groundwater exchanges vary between Sce21, Sce22 and Sce23 that can be deduced from the time required to reach the dynamic steady state, which increases with lower values of α'.

These results suggest that applying waterproof treatments to the walls could be counter-productive in terms of efficiency because higher efficiencies occur when the walls do not constrain the groundwater exchanges. An exception with respect to the time required to reach the dynamic steady state occurs if the walls are completely waterproof. In this case, the mid-range head difference remains constant and the BEP is reached immediately. However, it is difficult to completely isolate underground cavities because construction defects are relatively common [34–37]. The operation ranges of pumps and turbines would be higher with completely waterproof walls.

3.5. Storage capacity of the underground reservoir (V_{UR})

The results from four scenarios (Sce27 to Sce29) are compared to determine the importance of the storage capacity of the underground reservoir to the efficiency. The common features of the scenarios are as follows: K = 1 m/d, $\theta_S = 0.1$, α' = 1000 d^{-1}, and Hypothesis 1 is considered for the pumping and injection phases. The values of V_{UR} are 125,000 m^3 in Sce26, 250,000 m^3 in Sce27, 500,000 m^3 in Sce28 and 1,000,000 m^3 in Sce29. Note that only the storage capacity of the underground reservoir is modified to assess its influence separately. The geometry (i.e. size) is not varied to eliminate effects produced on the groundwater exchanges by an

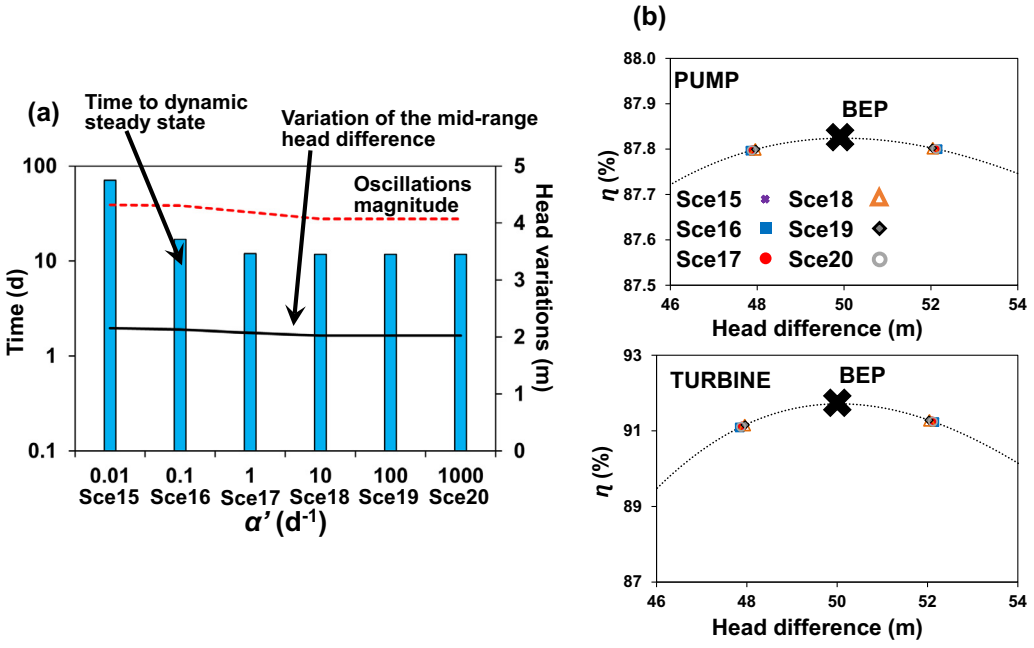

Fig. 9. (a) Head variations for 6 scenarios with different values of α'. The value of K of the porous medium is 10 m/d. (b) Operation range when the dynamic steady state is reached for the simulated scenarios.

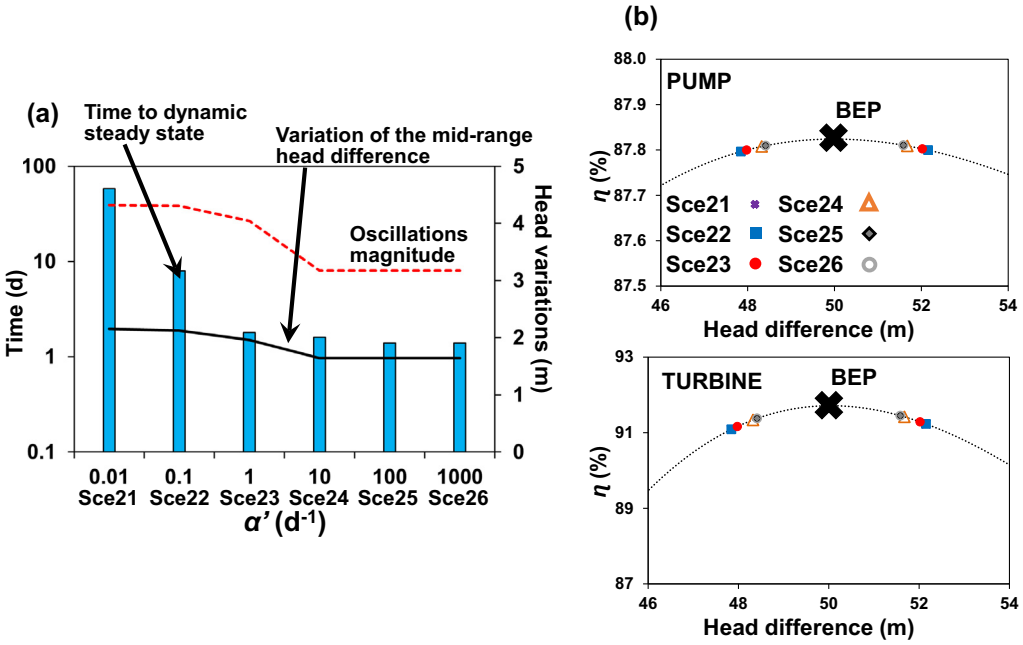

Fig. 10. (a) Head variations for 6 scenarios with different values of α'. The value of K of the porous medium is 100 m/d. (b) Operation range when the dynamic steady state is reached for the simulated scenarios.

increment of the exchange surface between the underground reservoir and the surrounding porous medium.

Fig. 11a shows the head variations, while Fig. 11b shows the operation ranges of the pumps and turbines. The variations of the mid-range head difference and the magnitude of the oscillations decrease significantly when larger storage capacities are considered. Conversely, the time to reach the dynamic steady state increases. Similarly, the size of the operation ranges decreases with larger storage capacities. The percentages of pumped or injected water that flows from or to the porous medium (i.e., groundwater exchanges) decrease with larger storage capacities. Thus, these results do not match with the previous ones because the efficiency increases with lower groundwater exchanges, which can be interpreted from the increase in the time to reach the dynamic steady state. In these scenarios, the decrease in efficiency associated to the reduction of the groundwater exchanges is compensated by the contraction of the operation ranges that occur when the storage capacity is increased keeping constants the pumping and injection rates.

3.6. Frequency of the pumping and injection intervals

The previous simulations were performed considering the continuous activity of the plant (Hypothesis 1). However, stops will

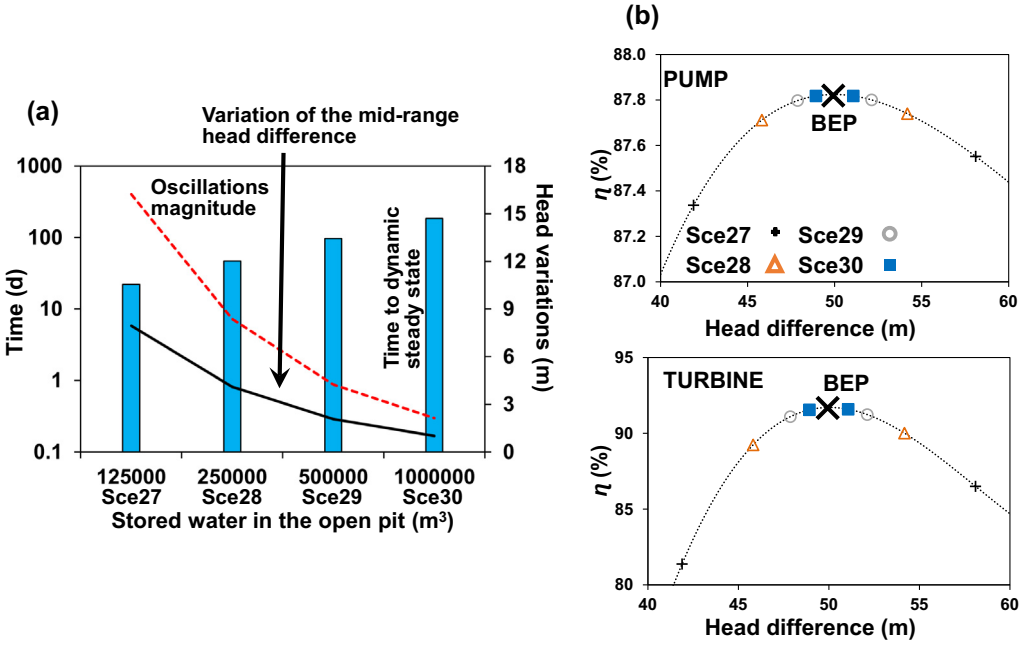

Fig. 11. (a) Head variations for 4 scenarios with different volumes of the underground reservoir. (b) Operation range when the dynamic steady state is reached for the simulated scenarios.

probably be common and required in UPSH plants to manage the electricity production. Five scenarios (Sce31 to Sce35) that differ in the frequency and the duration of the stops are compared. The common characteristics of the scenarios are as follows: $K = 1$ m/d, $\theta_S = 0.1$, $\alpha' = 1000\ d^{-1}$, $V_{UR} = 500{,}000\ m^3$, and Q_P and Q_I are 2 m^3/s. Sce31 is based on Hypothesis 1 (continuous pumping and injection), Sce32 is based on Hypothesis 2 (0.5 days of inactivity after each injection phase), Sce33 is based on Hypothesis 3 (0.5 days of inactivity after each pumping phase), Sce34 is based on Hypothesis 4 (1 day of inactivity after every two injections phases) and Sce35 is based on Hypothesis 5 (1 day of inactivity after every two pumping phases).

Fig. 12 summarizes the numerical results of Scenarios 31–35. The magnitude of the oscillations does not depend on the frequency and the duration of the period of inactivity. For this reason, the amplitudes of the operation ranges of the pumps and turbines are similar in all of the scenarios (Fig. 11b). The main differences in the head variations are the time required to reach the dynamic steady state and the variation of the mid-range head difference with time. On the one hand, more time is needed to reach the dynamic steady state when stops occur after the injection phases. This time decreases if the periods of inactivity are shorter. Thus, if the pumps and turbines are properly selected considering the final mid-range head difference, it would be advisable to carry out the periods of inactivity after pumping intervals. On the other hand, the variations of the mid-range head difference over time are greater when the stops occur after phases of pumping. Changes in the variation of the mid-range head difference are produced because the final value of the mid-range head difference with respect to the initial head difference between the reservoirs varies depending on the characteristics of the inactivity periods. While the final value of the mid-range head difference is the same as the initial head difference (before the UPSH plant starts operating) in Hypothesis 1, it is greater in Hypotheses 2 and 4 and smaller in Hypotheses 3 and 5. This fact must be carefully considered in the selection of pumps and turbines for future UPSH plants. If not, the pumps and turbines could operate far from their BEP. This behaviour and its consequences are shown more clearly in Fig. 12b. The relative position of the BEP (centred or not centred with respect to the operation range) varies depending on the hypothesis. The BEP is not located in the middle of the operation ranges in Sce31–34. The variation in the mid-range head difference from the initial conditions until the dynamic steady state is reached is smaller when the periods of inactivity occur after the injections and greater when the stops occur after pumping.

The efficiency of future UPSH plants can be improved by considering the characteristics of the expected and regular stops. If the value of the final mid-range head difference is adequately predicted and is considered in the selection of the pumps and turbines, the BEP will be centred with respect to the operation range. Note that the considered pumping/injection hypotheses are "simple" and predictable. However, they allow the main behaviours of the system to be ascertained. In real situations, the pumping/injection frequencies will be more heterogeneous.

3.7. Scale effects

The mean hydraulic power of the considered UPSH plant is 1 MW, which is not so much in comparison with actual PSH plants. Consequently, the scale effect on the results must be considered to establish if the influence of groundwater exchanges will be the same in larger UPSH plants. Higher hydraulic power will be reached by increasing the injection rate, which means (1) underground reservoirs with higher storage capacity or (2) higher head oscillations. If the increment of the storage capacity induces an increment of the exchange surface, groundwater exchanges will also increase (note that in this study the exchange surface is kept constant to assess only the influence of the storage capacity). If higher head oscillations are produced, groundwater exchanges will also increase because the hydraulic gradient between the porous medium and the reservoir will be higher. Higher hydraulic power could be also reached by planning the plant in a site with deeper underground reservoir and piezometric head. In this case, the influence of the groundwater exchanges on the efficiency will be the same.

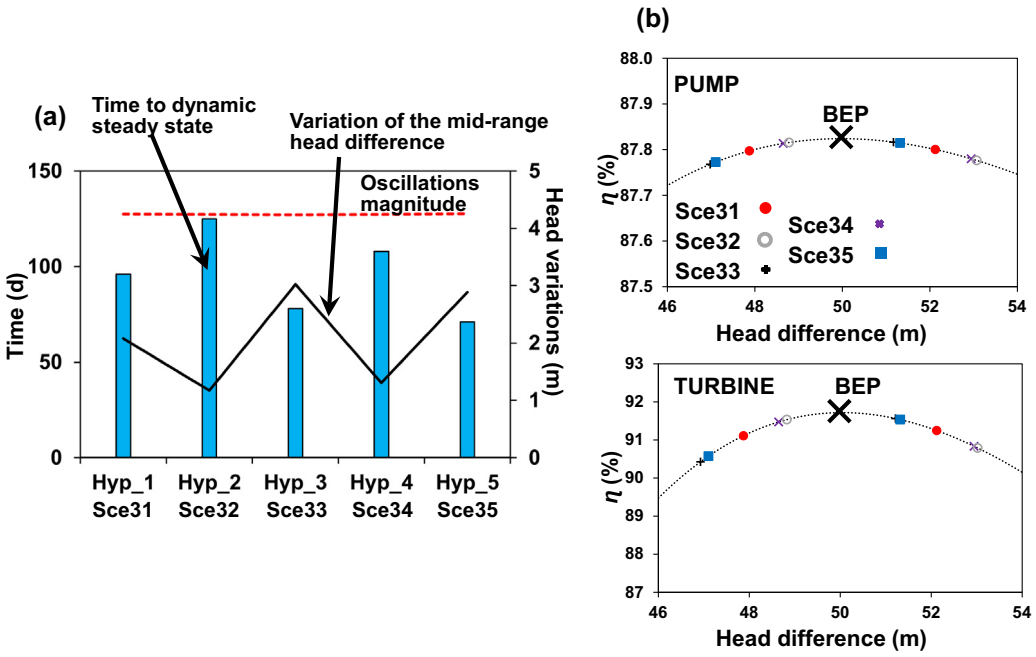

Fig. 12. (a) Head variations for 5 scenarios with different periods of inactivity. The characteristics are varied in each scenario. (b) Operation range when the dynamic steady state is reached for the simulated scenarios.

3.8. Environmental impacts

The Water Framework Directive [38] adopted by the European Union in October 2000 establishes that the nations must guarantee the good state of the groundwater bodies, and consequently, pollutants discharges into groundwater are forbidden. In the same manner, this directive states that reinjection of pumped water from mines and quarries is allowed if the discharges do not compromise previous environmental achievements. The most of future UPSH plants will respect the directive because pollutants will theoretically not be discharged since the water released to produce electricity will be that pumped previously. However, the environmental impacts must be rigorously investigated during the design stage of future UPSH plants because some of them could alter the groundwater quality. Piezometric head oscillations could mobilize contaminants contained in the unsaturated zone. In the same manner, hydrochemical modifications could be induced by the exposure of groundwater at the surface (i.e. oxidizing conditions) and further injection. Anyway, previous studies have demonstrated that environmental impacts would be higher as the groundwater exchanges increase [20,27,37]. Therefore, given that groundwater exchanges are not disadvantageous in terms of efficiency, an agreement should be achieved between the efficiency and the environmental impacts in future UPSH plants.

4. Summary and conclusions

Open pit mines, which can be used as underground reservoirs of UPSH plants, are rarely isolated. Consequently, water will flow in and out affecting the efficiency of the plant, which should be considered in its design. The main conclusions of this study are:

- Groundwater exchanges mitigate the head difference variations, which reduces the operation ranges of pumps and turbines. As a result, pumps/turbines operate at higher efficiency in UPSH plants than in classical PSH plants.
- Groundwater exchanges influence the evolution of the mid-range head difference over time, which must be considered in the selection of the pumps and turbines; otherwise, they could operate far from their BEPs.
- The time required to reach the dynamic steady state depends on the groundwater exchanges. This issue is important when long periods of inactivity, during which the head difference between the reservoirs returns to its initial value, occur because the pumps and turbines operate before around their BEPs if the dynamic steady state is reached more quickly.
- The frequency and duration of pumping, injection and periods of inactivity control the final mid-range head difference between the reservoirs, which must be considered to optimize the efficiency.
- The influence of groundwater exchanges on the efficiency decreases as the storage capacity of the underground reservoir increases. However, if a higher storage capacity implies a largest exchange surface, groundwater exchanges will continue to influence the efficiency.
- Water exchanges are not disadvantageous in terms of the efficiency; however, the environmental impacts on the surrounding porous medium are higher as the groundwater exchanges increase. Therefore, a compromise will be needed between the efficiency and the environmental impacts in future UPSH plants.

The variation of the efficiency that is caused by the groundwater exchanges when the dynamic steady state is reached is not too significant in this study. However, the influence of the groundwater exchanges will increase if the performance curves of the pumps and turbines are sharper.

Acknowledgements

E. Pujades gratefully acknowledges the financial support from the University of Liège and the EU through the Marie Curie BeIPD-COFUND postdoctoral fellowship programme (2014–2016 "Fellows from FP7-MSCA-COFUND, 600405"). S. Bodeux was supported by a research grant from FRIA (Fonds pour la Recherche dans l'Industrie et l'Agriculture, FRS-FNRS, Belgium). This research was supported by the Public Service of Wallonia – Department of Energy and Sustainable Building through the smartwater project.

References

[1] International Energy Agency (IEA). Key world energy trends, excerpt from: world energy balances, 2016.
[2] Hu Y, Bie Z, Ding T, Lin Y. An NSGA-II based multi-objective optimization for combined gas and electricity network expansion planning. Appl Energy 2016;167:280–93.
[3] Mileva A, Johnston J, Nelson JH, Kammen DM. Power system balancing for deep decarbonization of the electricity sector. Appl Energy 2016;162:1001–9.
[4] Okazaki T, Shirai Y, Nakamura T. Concept study of wind power utilizing direct thermal energy conversion and thermal energy storage. Renew Energy 2015;83:332–8.
[5] Athari MH, Ardehali MM. Operational performance of energy storage as function of electricity prices for on-grid hybrid renewable energy system by optimized fuzzy logic controller. Renewable Energy 2016;85:890–902.
[6] Giordano N, Comina C, Mandrone G. Borehole thermal energy storage (BTES). First results from the injection phase of a living lab in Torino (NW Italy). Renew Energy 2016;86:993–1008.
[7] Gebretsadik Y, Fant C, Strzepek K, Arndt C. Optimized reservoir operation model of regional wind and hydro power integration case study: Zambezi basin and South Africa. Appl Energy 2016;161:574–82.
[8] Mason IG. Comparative impacts of wind and photovoltaic generation on energy storage for small islanded electricity systems. Renew Energy 2015;80:793–805.
[9] Delfanti M, Falabretti D, Merlo M. Energy storage for PV power plant dispatching. Renew Energy 2015;80:61–72.
[10] Zhang N, Lu X, McElroy MB, Nielsen CP, Chen X, Deng Y, et al. Reducing curtailment of wind electricity in China by employing electric boilers for heat and pumped hydro for energy storage. Appl Energy 2016;184:987–94.
[11] Steffen B. Prospects for pumped-hydro storage in Germany. Energy Policy 2012;45:420–9.
[12] Chen H, Cong TN, Yang W, Tan C, Li Y, Ding Y. Progress in electrical energy storage system: a critical review. Prog Nat Sci 2009;19(3):291–312.
[13] Mueller SC, Sandner PG, Welpe IM. Monitoring innovation in electrochemical energy storage technologies: a patent-based approach. Appl Energy 2015;137:537–44.
[14] Wong IH. An underground pumped storage scheme in the bukit Timah granite of Singapore. Tunn Undergr Space Technol 1996;11(4):485–9.
[15] Kucukali S. Finding the most suitable existing hydropower reservoirs for the development of pumped-storage schemes: an integrated approach. Renew Sustain Energy Rev 2014;37:502–8.
[16] Uddin N. Preliminary design of an underground reservoir for pumped storage. Geotech Geol Eng 2003;21:331–55.
[17] Meyer F. Storing wind energy underground. Eggenstein Leopoldshafen, Germany: FIZ Karlsruhe – Leibnz Institute For Information Infrastructure; 2013. ISSN: 0937–8367.
[18] Madlener R, Specht JM. 2013. An exploratory economic analysis of underground pumped-storage hydro power plants in abandoned coal mines. FCN Working Paper No. 2/2013.
[19] Alvarado R, Niemann A, Wortberg T. Underground pumped-storage hydroelectricity using existing coal mining infrastructure. In: E-proceedings of the 36th IAHR world congress, 28 June–3 July, 2015. the Netherlands: The Hague; 2015.
[20] Bodeux S, Pujades E, Orban P, Brouyère S, Dassargues A. Interactions between groundwater and the cavity of an old slate mine used as lower reservoir of an UPSH (Underground Pumped Storage Hydroelectricity): a modelling approach. Eng Geol 2016. http://dx.doi.org/10.1016/j.enggeo.2016.12.007.
[21] Braat KB, Van Lohuizen HPS, De Haan JF. Underground pumped hydro-storage project for the Netherlands. Tunnels Tunneling 1985;17(11):19–22.
[22] Spriet J. A Feasibility study of pumped hydropower energy storage systems in underground cavities MSc thesis, 2013.
[23] Severson MJ. Preliminary evaluation of establishing an underground taconite mine, to be used later as a lower reservoir in a pumped hydro energy storage facility, on the Mesabi iron range. Minnesota: Natural Resources Research Institute, University of Minnesota, Duluth, MN, Report of Investigation NRRI/RI-2011/02; 2011. 28 p.

[24] Niemann A. Machbarkeitsstudie zur Nutzung von Anlagen des Steinkohlebergbaus als Pumpspeicherwerke. Conference talk held at: Pumpspeicherkraftwerke unter Tage: Chance für das Ruhrgebiet, 2011–11-30, Essen, Germany; 2011. <www.uni-due.de/wasserbau>.
[25] Beck HP, Schmidt M, editors. Windenergiespeicherung durch Nachnutzung stillgelegter Bergwerke.
[26] Luick H, Niemann A, Perau E, Schreiber U. Coalmines as Underground Pumped Storage Power Plants (UPP) – a contribution to a sustainable energy supply? Geophys Res Abstr 2012;14:4205.
[27] Pujades E, Thibault W, Bodeux S, Philippe O, Dassargues A. Underground pumped storage hydroelectricity using abandoned works (deep mines or open pits) and the impact on groundwater flow. Hydrogeol J 2016. http://dx.doi.org/10.1007/s10040-016-1413-z.
[28] Denimal S, Bertrand C, Mudry J, Paquette Y, Hochart M, Steinmann M. Evolution of the aqueous geochemistry of mine pit lakes – Blanzy–Montceau-les-Mines coal basin (Massif Central, France): origin of sulfate contents; effects of stratification on water quality. Appl Geochem 2005;20(5):825–39.
[29] Brouyère S, Orban Ph, Wildemeersch S, Couturier J, Gardin N, Dassargues A. The hybrid finite element mixing cell method: A new flexible method for modelling mine ground water problems. Mine Water Environ 2009. http://dx.doi.org/10.1007/s10230-009-0069-5.
[30] Wildemeersch S, Brouyère S, Orban Ph, Couturier J, Dingelstadt C, Veschkens M, et al. Application of the hybrid finite element mixing cell method to an abandoned coalfield in Belgium. J Hydrol 2010;392:188–200.
[31] Celia MA, Bouloutas ET, Zarba RL. A general mass conservative numerical solution for the unsaturated flow equation. Water Resour Res 1990;26:1483–96.
[32] Orban Ph, Brouyère S. Groundwater flow and transport delivered for groundwater quality trend forecasting by TREND T2, Deliverable R3.178, AquaTerra project; 2006.
[33] Chapallaz JM, Eichenberger P, Fischer G. Manual on pumps used as turbines. Braunschweig: Vieweg; 1992.
[34] Bruce D, De Paoli B, Mascardi C, Mongilardi E. Monitoring and quality control of a 100 m deep diaphragm wall. In: Burland J, Mitchell J, editors. Pilling and deep foundations. Rotterdam: A.A Balkema; 1989. p. 23–32.
[35] Vilarrasa V, Carrera J, Jurado A, Pujades E, Vazquez-Sune E. A methodology for characterizing the hydraulic effectiveness of an annular low-permeability barrier. Eng Geol 2011;120:68–80.
[36] Pujades E, Carrera J, Vàzquez-Suñé E, Jurado A, Vilarrasa V, Mascuñano-Salvador E. Hydraulic characterization of diaphragm walls for cut and cover tunnelling. Eng Geol 2012;125:1–10.
[37] Pujades E, Jurado A, Carrera J, Vázquez-Suñé E, Dassargues A. Hydrogeological assessment of non-linear underground enclosures. Eng Geol 2016;207:91–102.
[38] Water Framework Directive, Water Framework Directive, 2000/60/EC. Eur. Commun. Off. J.; L327.22.12.2000.